Study on Thermal Crack Characteristics of Granite in Shandong Province, China under Different Temperatures and Heating/Cooling Treatments

Weiqiang Zhang *, Wei Li , Xin Zhang , Wei Qiao , Yangzhou Wang , Jinyu Xie

Posted Date: 6 September 2023

doi: 10.20944/preprints202309.0381.v1

Keywords: granite; thermal crack; high temperature; heating/cooling path; crack mechanism

Article

Study on Thermal Crack Characteristics of Granite in Shandong Province, China under Different Temperatures and Heating/Cooling Treatments

Weiqiang Zhang [1,2,*], Wei Li [2], Xin Zhang [2,3], Qiao Wei [1,2,4], Yangzhou Wang [1,4] and Jingyu Xie [1,2]

[1] School of resources and Earth Sciences, China University of mining and technology, Xuzhou, Jiangsu, 221116, P.R. China
[2] Shandong energy group, Jinan, Shandong, 250101，P.R. China
[3] China University of Petroleum (Huadong), Qingdao, Shandong, 266580, P.R. China
[4] South America Co., Ltd of Shandong energy group, Qingdao, Shandong, 266000, P.R. China
* Correspondence: Tel:+86-1589-6427-723, zhangweiqiang1204@163.com.

Abstract: The upgrading of energy structure is an important issue that restricts the sustained and rapid development of China's economy, among which the research and development of renewable and clean energy is an important lever. At present, the clean energy with recoverable technology and huge reserves is hot dry rock geothermal resources, but the key factor restricting its commercial development is reservoir fracturing technology. The thermal crack mechanism of granite studied in this paper is the foundation for the transformation of hot dry rock reservoirs. In order to deeply study the thermal crack mechanism of rock, this paper conducted thermal cracking experiments on granite at different temperatures and heating/cooling paths, and qualitative and quantitative analysis was conducted on the crack initiation characteristics, propagation paths, and crack network morphology of rock thermal crack under different test conditions. The thermal crack mechanism was also analyzed from the perspectives of mineral petrology, fracture mechanics, thermodynamics, and other aspects. The research results show that there are two obvious mutation points in the study temperature range for samples with fast cooling paths (SF path: slow heating and fast cooling; FF path: fast heating and fast cooling), around 200-300 ℃ and 600 ℃, respectively, while for samples with slow cooling paths (SS path: slow heating and slow cooling; FS path: fast heating and slow cooling), there is only one mutation point around 600 ℃. The initiation positions of thermal cracking under all temperature paths are relatively similar, with intergranular crack located between particles at the edge of the sample or intercrystalline crack in the middle of feldspar or quartz aggregates. The initiation temperature of SF and FF path specimens is relatively low compared to SS and FS path specimens, and the number and size of cracks is small. The crack network structure formed by the SF path is the most complex, with the largest crack ratio and cumulative crack length; The crack network structure formed by the FF path is relatively complex, with a larger main crack size but relatively fewer secondary cracks; The FS and SS paths do not form a complex network with good connectivity. The process of thermal crack development can be divided into three stages: the development of small cracks, the joint development of main cracks and small cracks, and the connection of cracks into a network structure. The mechanism of thermal crack propagation is that the expansion and thermal conductivity between different crystals are different. The thermal stress caused by temperature gradient and the tension or shear stress caused by the inconsistent deformation of crystals form stress concentration in weak areas such as particles boundary, cleavage, and original cracks. Firstly, it causes some crystals with smaller strength or less rounded shape to crack, and when the combined stress is large, the cracks will gradually expand along the existing fine cracks. This also explains that the most main cracks of the SF and FF path specimens mainly surround some large mineral aggregates or between particles. The results are the foundation for sustainable development and can support key technological breakthroughs in hot dry rock development.

Keywords: granite; thermal crack; high temperature; heating/cooling path; crack mechanism

 doi:10.20944/preprints202309.0381.v1

1. Introduction

After subjecting to high temperature, thermal cracks are likely to occur inside and outside the rock, which can change the physical and mechanical properties of the rock and lead to some potential disasters in hot dry rock development, geological storage of high radioactive nuclear waste and underground coal gasification [1-5]. On the other hand, some deep underground projects such as the development of oil, gas, and geothermal resources also require fracturing to create a certain volume of complex fracture networks to increase the seepage of oil, gas, or heating media [6-8]. Therefore, conducting research on the thermal crack mechanism of rocks has important theoretical significance and engineering application value.

At present, the reported research on rock thermal crack mainly focuses on thermal damage experiments, microscopic test of rocks under and after high temperatures, and numerical simulations [9-13]. Theoretical research is rare [14-15]. The thermal damage experiment is mainly test the response characteristics of rock structural damage in terms of physical and mechanical properties under high temperature effect, such as the influence of high temperature on rock strength, density, permeability, wave velocity, elastic modulus and other parameters [16-18]. The research results indicate that linear expansion coefficient, Poisson's ratio, and peak strain increase with increasing temperature, while permeability, compressive strength, wave velocity, and elastic modulus decrease with increasing temperature. The temperature range of 300-500 ℃ is the temperature range where the change rate of most parameters changes abruptly. There are few direct observation instruments for rock crack under real-time conditions of high temperature and pressure, especially for temperatures above 200 ℃ [19]. The microscopic study of rock thermal crack mainly relies on advanced microscopic testing equipment such as scanning electron microscope, optical microscope, nuclear magnetic resonance instrument, CT scanner, etc [20-23]. Among them, scanning electron microscope and optical microscope can directly qualitatively observe the crack degree; Nuclear magnetic resonance can effectively study the total amount of cracks and the distribution of crack with different size; CT scanning can quantitatively study the initiation and development process of cracks, but the testing cost is high, and the testing accuracy is directly related to the sample size. The numerical simulation research of rock thermal crack mainly focuses on the fracture deformation of rocks, studying the distribution characteristics of stress and deformation fields around cracks [24-25]. This can provide a basis for the mechanism of thermal crack, but it cannot be fully consistent with the actual fracture situation. In addition, some scholars have established some simplified solid-thermal coupling mathematical models to explore the temperature threshold of thermal crack and the conditions for different crack propagation paths in theory [26-27]. Based on the above analysis, it can be seen that there has been many research on rock thermal crack, but the main purpose of the research is to provide mechanism analysis for the variation of macroscopic physical and mechanical properties. The research on the initiation, propagation, influencing factors, and mechanism of thermal crack is not comprehensive, and a large amount of research needs to be carried out. In addition, the heating/cooling path also has a significant impact on rock thermal crack. Previous research has mostly focused on thermal crack under specific paths [28-30], and it is necessary to supplement the mechanisms of rock thermal crack under different heating/cooling paths.

In response to the above problems, this paper selected typical granite in deep strata as the research object, conducted thermal crack tests at different temperatures and heating/cooling paths, observed the initiation and propagation laws of thermal crack under different test conditions, analyzed the structural characteristics of fracture network under different heating/cooling paths, and finally revealed the mechanism of thermal crack development based on mineral petrology, fracture mechanics, thermodynamics, and other perspectives. The research results can serve rock engineering related to high-temperature environments such as hot dry rock development, underground coal gasification, and geological storage of nuclear waste.

Preprints (www.preprints.org) | NOT PEER-REVIEWED | Posted: 6 September 2023 doi:10.20944/preprints202309.0381.v1

2. Sample preparation and experimental methods

The granite samples were taken from Shandong Province, China, with average density of 2.68 g/cm3. The apparent colors are mainly white, flesh red, and black. According to the analysis of X-ray diffraction (XRD) (Figure 1), the main mineral composition of the samples was quartz, albite, K-feldspar and hornblende. Due to the majority of mineral particles with high crystallinity have sizes between 1-5mm, it is determined that the test sample is medium grained granite. The test samples were cut into cylinder samples with a diameter of 25 mm and a height of 20 mm. The height error was controlled within 0.5 mm, and the diameter error was ensured to be less than 0.3 mm. The samples were placed under a magnifying glass to check the cracks on their surfaces, which helped select the test samples with no macroscopical crack.

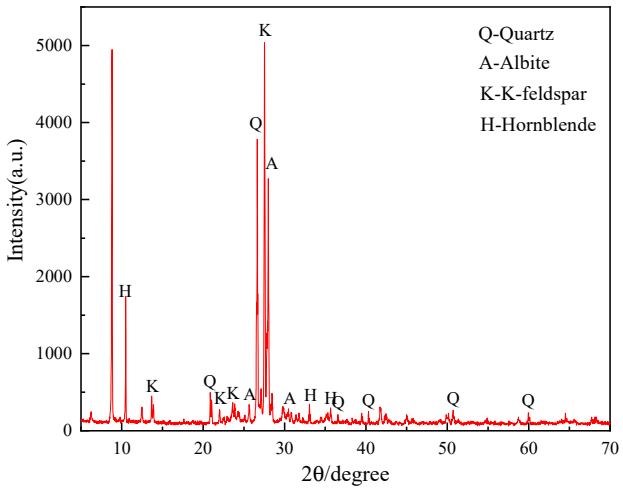

Figure 1. Analysis results of main mineral components of samples based on x-ray diffraction test.

Group the selected samples and first perform high-temperature treatment under different temperature and heating/cooling path in an mf6000 high-temperature intelligent muffle furnace. A total of 9 temperature levels and 4 heating/cooling paths were set for this test, as shown in Table 1. Each test condition set two parallel samples.

Table 1. Summary of the four heating/cooling processes (heating treatments).

Test method	Heating process	Target temperature	Holding time	Cooling process
SS treatment	slow heating (10 ℃/min)	100 ℃、200 ℃、……800 ℃	2 h	slow cooling (Natural cooling in air at room temperature)
SF treatment	slow heating (10 ℃/min)	100 ℃、200 ℃、……800 ℃	2 h	fast cooling (Put it into 20 ℃ water to cool down)
FS treatment	fast heating (30 ℃/min)	100 ℃、200 ℃、……800 ℃	2 h	slow cooling (Natural cooling in air at room temperature)
FF treatment	fast heating (30 ℃/min)	100 ℃、200 ℃、……800 ℃	2 h	fast cooling (Put it into 20 ℃ water to cool down)

After the sample undergoes high-temperature treatment, the apparent morphology of the sample is photographed using a stereoscope and a digital camera. Then the microscopic and macroscopic crack conditions of the sample surface can be obtained, and the initial temperature, initiation site, propagation path, and complexity of the crack can be qualitatively analyzed. In order to deeply analyze the thermal crack mechanism of rocks, crack image processing system (CIAS) developed by Nanjing University is referenced to process crack information in images, which can

Preprints (www.preprints.org) | NOT PEER-REVIEWED | Posted: 6 September 2023 doi:10.20944/preprints202309.0381.v1

quickly acquire various quantized geometric information of cracks and blocks from crack images, including crack nodes, endpoints, crack numbers and statistical parameters such as single crack length, total crack length, the average width of a single crack, the average width of all cracks, single crack area, total crack area, crack rate, crack fractal dimension, single block area, block perimeter and shape coefficient. The microscopic pictures can deeply analyze the mechanism of thermal crack of rocks from the perspective of mineral Petrology. The test process is shown in Figure 2.

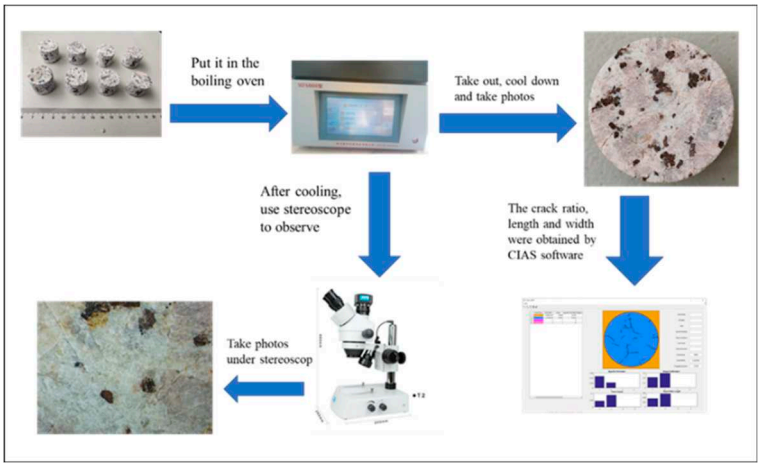

Figure 2. Schematic diagram of testing equipment and process.

3. Experimental results and analysis

Based on the above experiments, the initiation characteristics, propagation patterns, and fracture network morphology of granite samples subjected to different temperatures and temperature rise and fall paths were obtained. The main experimental results are as follows.

3.1. Initiation characteristics of thermal crack

The macroscopic characteristics of the samples change continuously after high-temperature treatments are shown in Figure 3.a, and the Figure 3.b shows the schematic diagram of the thermal crack propagation process. From Figure 3, it can be seen that thermal cracking gradually occurs on the surface of granite samples as the temperature increases, while the initiation temperature and position of thermal cracks under different temperature paths are significant differences. The initiation temperature of the samples under SS and FS paths is around 600 ℃, while the initiation temperature of the samples under FS and FF paths is around 300 ℃ and 200 ℃, respectively. This indicates that the heating rates of 10 ℃/min and 30 ℃/min used in the experiment have little effect on the thermal cracking of granite, while the cooling rate (cooling in air at room temperature or cooling in 20 ℃ water) have a greater impact on the thermal cracking of the sample.

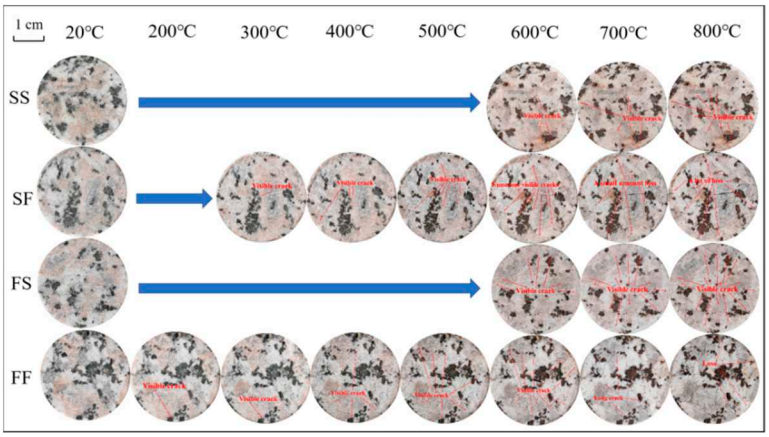

(a) The development process of thermal crack of rock surface with temperature

Preprints (www.preprints.org) | NOT PEER-REVIEWED | Posted: 6 September 2023 doi:10.20944/preprints202309.0381.v1

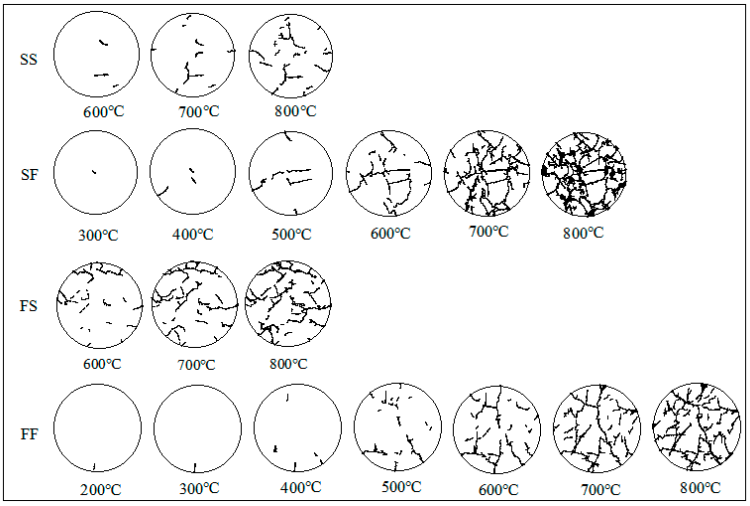

(b) Schematic diagram of rock thermal crack propagation process

Figure 3. The macroscopic change of thermal cracks of the granite samples.

The initiation positions of thermal crack of granite samples are shown in Figure 4, and which shows that the initiation positions of samples under different temperature paths are relatively similar and can be basically divided into two categories: ① Intergranular crack: located at the boundary between mineral particles, such as the junction of small amphibole and quartz or feldspar (which are often found at the edge of the sample); the junction between feldspar, quartz or amphibole aggregates (which is mostly located in the middle of the sample); ② Intercrystalline crack: located in the feldspar or quartz aggregates, and it is found at both the edge and middle of the samples, but more in the middle. The number of initiation thermal cracks in granite samples can be seen in Figure 3.b , and which indicates that the temperature path has a significant impact on it. The two paths of rapid cooling (SF and FF path) have lower initiation temperatures for thermal cracking of specimens, while the number of initiation thermal cracks is very small. On the contrary, the slowly cooled (FS and SS path) samples have a relatively high initiation temperature for thermal cracking, but there are relatively more initiation thermal cracks. Among them, the FS path samples have the most initiation thermal cracks. Although the threshold temperature for the thermal cracking of samples under SS path is consistent with the FS path samples, the number of initiation thermal cracks is significantly higher. Comparing the samples with four heating/cooling paths at the same temperature(such as 600 °C), found that although the samples with a slow cooling path has a higher number of initiation thermal cracks, the finally number of thermal cracks is less than that of samples with a rapid cooling path, and the heating/cooling paths with the highest to lowest number of thermal cracks are FF, SF, FS, and SS path. This also indicates that a high temperature difference will cause greater thermal stress inside the samples and make it easier to form stress concentration.

Preprints (www.preprints.org) | NOT PEER-REVIEWED | Posted: 6 September 2023 doi:10.20944/preprints202309.0381.v1

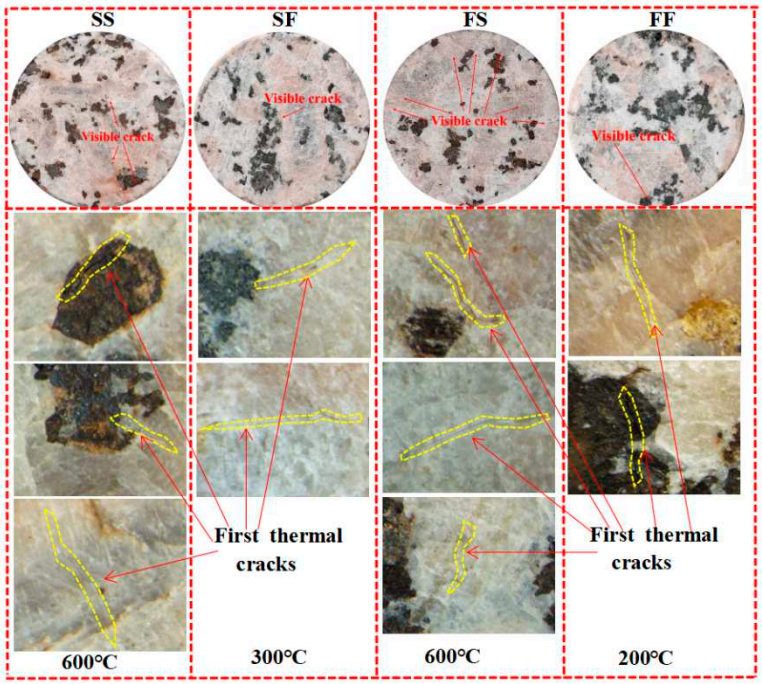

Figure 4. The position of first thermal cracks under different heating/cooling paths.

3.2. Propagation process of thermal cracks with temperature

Not only do the initiation characteristics of thermal cracks in granite samples differ significantly under different heating temperatures and heating/cooling paths, but also the propagation characteristics of thermal cracks. Figure 3 qualitatively shows the propagation process of thermal cracking, which indicates that the number of thermal cracks in the samples under four heating/cooling paths gradually increases with the increase of the target temperature, but the growth rate of the length, width, and quantity of cracks are significant differences. During the thermal cracking process, it can be observed that 600 ℃ is a significant mutation threshold temperature. The samples under SS and FS path did not undergo thermal cracking before 600 ℃, and thermal cracking gradually developed above 600 ℃ (as shown in Figure 3a). For the samples under SF and FF path, although the thermal cracking occurs around 200 or 300 ℃, the development below 600 ℃ are very slow, and the thermal cracks are mostly small cracks that occur randomly. When the temperature above 600 ℃, the development rate of thermal cracking significantly increases, as shown in Figure 3a. It is worth noting that the heating/cooling paths of the samples with the growth rate from large to small above 600 ℃ are SF, FF, FS and SS, respectively. This is because rock is a poor conductor of heat, and the temperature difference in the cooling process is significantly greater than that in the heating process. At the same time, the heating time in the SF path is longer than that in the FF path, resulting in a longer heating time for the SF sample and a faster rate of thermal cracking during the rapid cooling process.

On the basis of the above qualitative analysis, the crack ratio, total crack length, and average crack width during the thermal cracking process were quantitatively processed using CIAS software, as shown in Figure 5, and the calculation formula for the above three parameters are shown in Eq. (1), (2) and (3).

$$\nu = \frac{S_c}{S} \times 100\% \tag{1}$$

$$L_t = \sum_{1}^{n} L_i \tag{2}$$

Preprints (www.preprints.org) | NOT PEER-REVIEWED | Posted: 6 September 2023 doi:10.20944/preprints202309.0381.v1

$$W = \frac{\sum_{1}^{n} W_i}{n} \tag{3}$$

Where, ν is the crack ratio; S_c the area of thermal cracks, mm²; S is the area of sample, mm²; L_t is the cumulative length of thermal cracks, mm; L_i is the length of the i-th thermal crack, mm; W is the average width of the thermal cracks, mm; W_i is the length of the i-th thermal crack, mm.

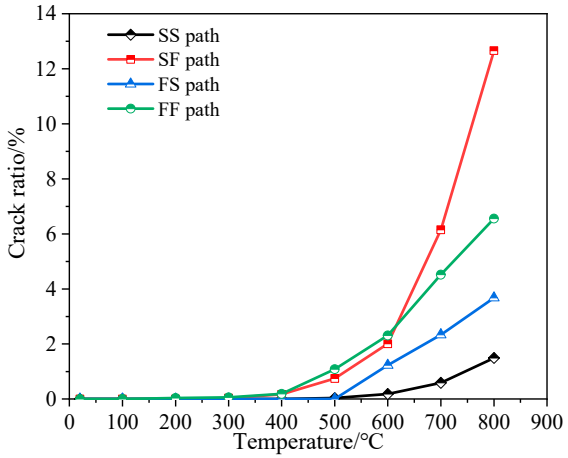

(a) Crack ratio of samples heated by different temperatures

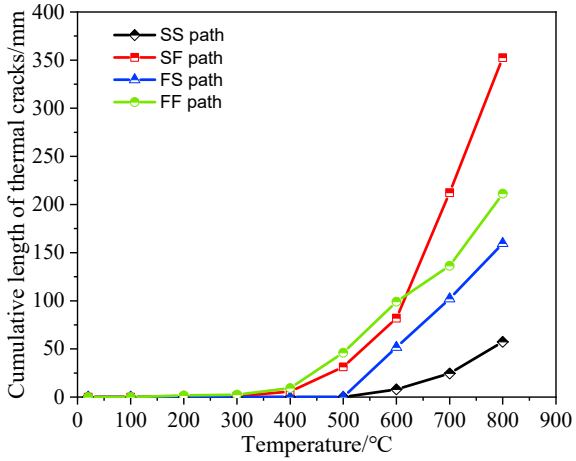

(b) Cumulative length of thermal cracks in different temperatures

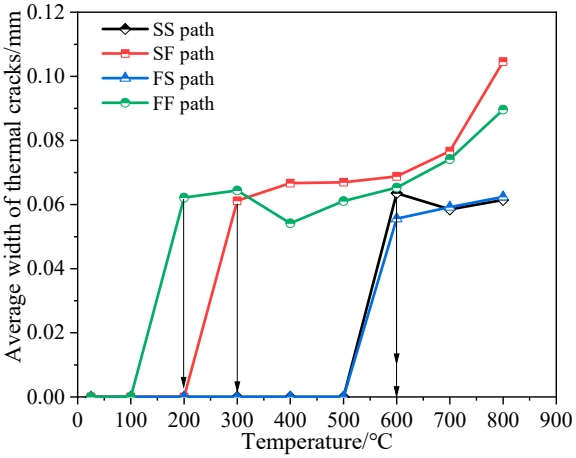

(c) Average width of thermal cracks in different temperatures

 doi:10.20944/preprints202309.0381.v1

Figure 5. Quantitative process of thermal cracking in granite samples under high temperature.

The crack ratio can comprehensively reflect the development rate of thermal fracture in granite samples, and the total length and average width of thermal cracks can reflect the characteristics of crack development at different stages during the progressive process of thermal cracking. Due to the interconnectivity of thermal cracks during the develop process, the number of thermal cracks in the analysis process is relatively complex, and the changes in the number of thermal cracks are not directly analyzed. Figure 5 shows the variation curve of the crack ratio of the samples with heating temperature, which indicating that the heating/cooling path has a significant impact on the degree of thermal cracking. The crack ratio values of the samples under 800 ℃ and four heating/cooling paths vary greatly, and with the order from large to small being SF, FF, FS and SS path, respectively. The difference between the maximum and minimum values is about 8.5 times. From the perspective of change rate, there is a basically identical inflection point near 600 ℃ for the four curves. Before the inflection point, the crack ratio growth rate of the SF and FF path samples is very slow, while the crack ratio data of the SS and FS path samples is not extracted; After the inflection point, the rate of change in the crack ratio of the SF and FF path samples is significantly accelerated, and the crack ratio of the SS and FS path samples begins to slowly increase. In which, the samples under SF and FF paths has the fastest change rate, the samples under SS path has the smallest rate of change, and the sample under FS path has a moderate change rate.

Comparing the curves in Figure 5.a and Figure 5.b, it can be seen that the change of cumulative length of thermal cracks is similar to that of the crack ratio. By comprehensive analysis of Figure 5, the characteristics of thermal fracturing development within different temperature ranges can be obtained. For the samples under SS path, thermal cracking began to be observed at 600 ℃, and the average width of cracks decreased between 600 and 700 ℃, while it slightly increased between 700 and 800 ℃. The crack ratio and number of cracks slowly increased between 600 and 800 ℃. This indicating that the thermal cracking developed between 600 and 700 ℃ is a thin crack with a very small width, and the original crack width increased after 700 ℃. For the samples under FS path, the crack ratio, cumulative length and average width of thermal cracks all show an approximate linear increase above 600 ℃, indicating that the width of the most of subsequent developed thermal cracks is larger than the initial cracks, and the size of existing cracks is gradually increasing. The average width curves of the SF and FF path samples are also very similar, with little change below 600 ℃ and a rapid increase above 600 ℃. This indicates that the thermal cracks developed in the samples of these two heating/cooling paths below 600 ℃ are mainly small cracks, while larger thermal cracks gradually develop above 600 ℃. In order to gain a clearer understanding of the thermal cracking characteristics under different temperature effects, the distribution of the length of thermal cracks with different widths in the cumulative length at different temperatures was calculated, and the results as shown in Figure 6. Note that the samples of SS and FS paths did not exhibit thermal cracks with a width greater than 0.075mm before 600 ℃, and only developed thermal cracks with a width between 0.075 and 0.1mm at 800 ℃. The width of thermal cracks developed in the samples under FF path is less than 0.075mm below 400 ℃,and a small number of thermal cracks with a width between 0.075 and 0.01mm were developed at 500 ℃. At 700 ℃, thermal cracks with a width between 0.1 and 0.3mm were developed. Only a small number of thermal cracks with a width greater than 0.3mm were developed at 800 ℃. For specimens under SF paths, the order and pattern of thermal cracks with different width are basically consistent with the samples under FF paths, but cracks with widths between 0.1 and 0.3mm occur at relatively low temperatures, and the length of thermal cracks with larger widths accounts for a larger proportion at the same temperature.

Preprints (www.preprints.org) | NOT PEER-REVIEWED | Posted: 6 September 2023 doi:10.20944/preprints202309.0381.v1

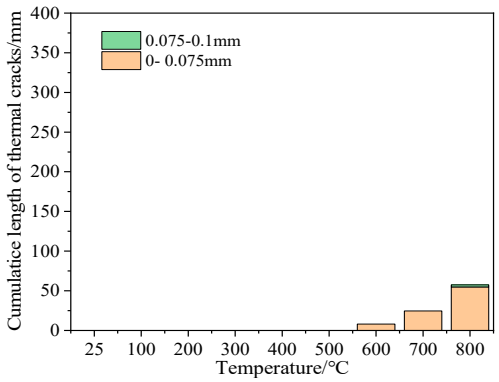

(a) SS path

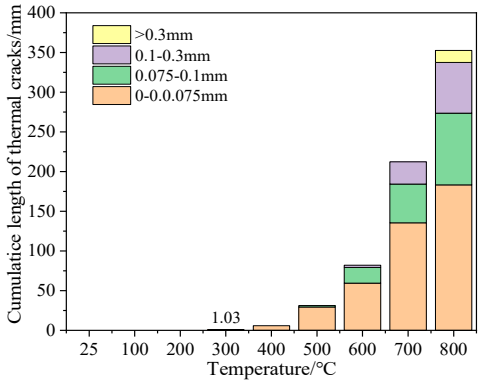

(b) SF path

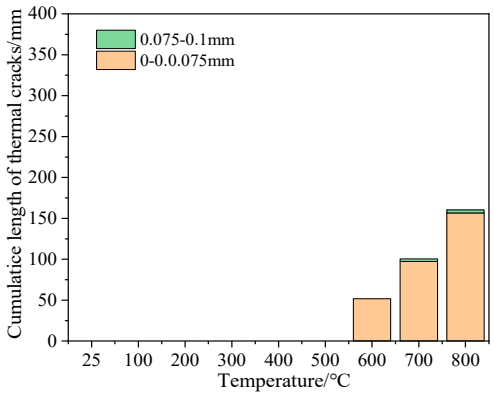

(c) FS path

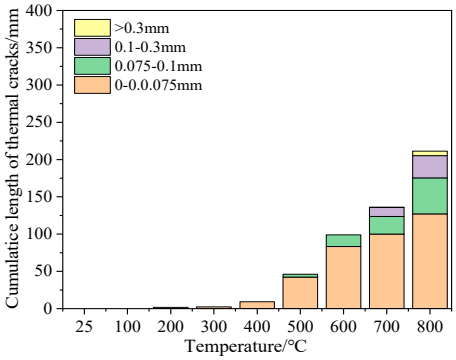

(d) FF path

Figure 6. The length distribution of thermal cracks with various width.

3.3. Apparent morphological characteristics

Under different temperatures and heating/cooling paths, granite samples exhibit varying degrees of thermal cracking, resulting in different apparent morphological characteristics. At the same temperature, the most complex apparent thermal crack network is the SF path, followed by FF,

 doi:10.20944/preprints202309.0381.v1

FS, and SS path. The apparent morphology of granite samples subjected to 800 °C under four different heating/cooling paths is shown in Figure 7, which shows that the apparent morphology of the rock samples under SS and FS paths did not undergo significant changes, and the length and width of the developed thermal cracks were smaller, with a few cracks interconnected. Among them, the number, length, and width of cracks in the FS path specimen are slightly larger than those in the SS path specimen. The apparent morphology of the samples under SF and FF paths has undergone significant changes, with not only a large number of developed thermal cracks, but also a significant increase in crack length and width compared to the samples under SS and FS paths. It is worth noting that under these two heating/cooling paths, the surface of the samples forms a complex network of connected thermal cracks, and several thermal cracks with larger lengths and widths form a framework of the crack network, which can named the main crack. There are some secondary thermal cracks with relatively small length and width developed between the main cracks, which make them interconnected. In addition, the complex network of thermal cracks cuts the sample, causing some smaller fragments to fall and form small pits, which disrupts the integrity of the sample morphology.

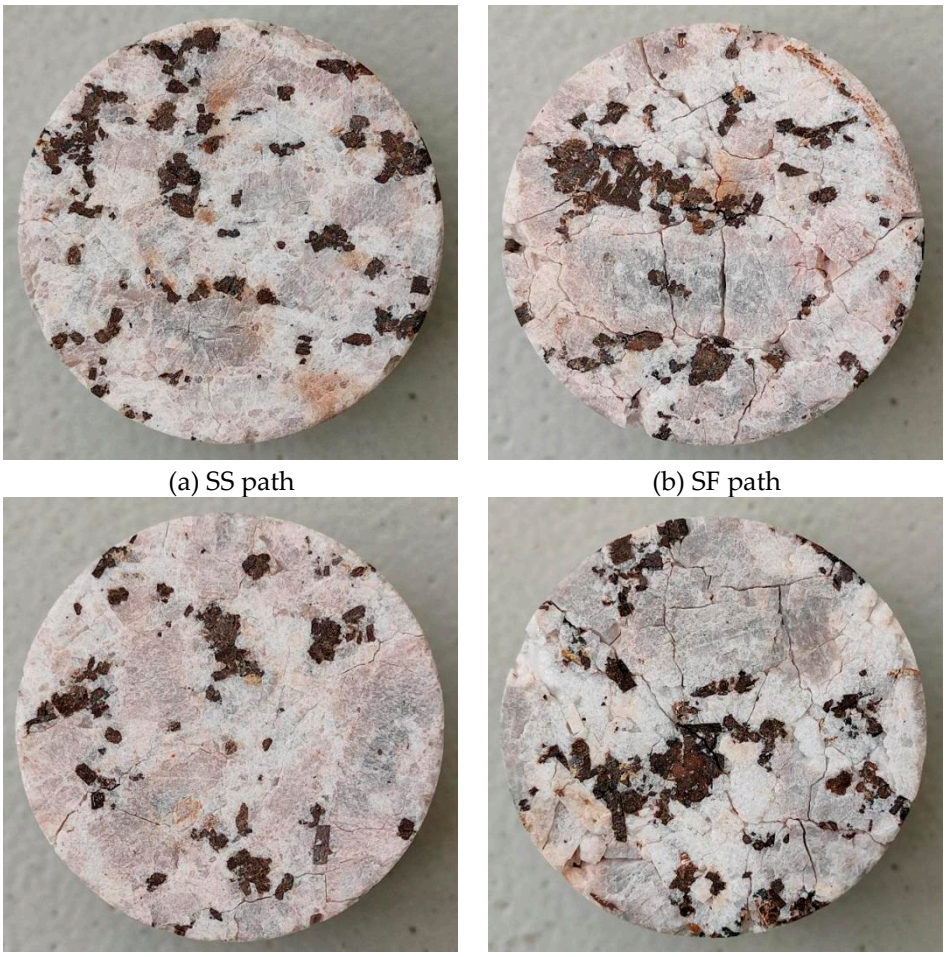

(a) SS path (b) SF path

(c) FS path (d) FF path

Figure 7. The apparent morphological characteristics of granite samples after experiencing 800 with different heating/cooling paths.

Through the analysis of the surface morphology characteristics of the samples, it was found that the heating/cooling path has a significant impact on the complexity of the thermal crack network. For example, rapid heating/cooling path can form some larger cracks, but there are relatively fewer secondary cracks between the main thermal cracks; Slow heating and rapid cooling can form a very complex network of cracks, with many secondary cracks developing between the main cracks, which is beneficial for the desorption and migration of gas resources in the rock mass. Slower cooling path can slight increase the permeability of rock, and have little impact on the physical and mechanical

 doi:10.20944/preprints202309.0381.v1

properties. This has reference significance for the controllable fracturing of reservoirs in deep geothermal development and shale gas development.

4. Discussion

Thermal crack is the basic phenomenon of rock thermal damage and an important factor affecting rock physical and mechanical properties [18]. At present, the common understanding of the mechanism of rock thermal crack is that the difference in thermal expansion coefficients and deformation properties of different minerals causes thermal stress, and when the thermal stress exceeds the strength of minerals or mineral aggregates, thermal crack occurs[18, 28]. Furthermore, the physical and chemical reactions such as rock dehydration, dehydroxylation, and mineral decomposition under high temperature can lead to the concentration of thermal stress at the defect site, exacerbating the development and expansion of thermal crack [21, 31].

Previous studies have shown that the main mineral components (such as quartz, feldspar, pyroxene, and mica) in granite do not change within 800 ℃ [18, 31]. However, there are small changes in the phase transitions and valence states of some minerals during heating process. The mineral phase transition is mainly reversible between α-quartz and β-quartz around 573 ℃. Although this phase transition does not cause changes in mineral composition, it can cause severe volume expansion, leading to rapid development of thermal crack. The change in the valence state of some mineral elements mainly causes a change in the apparent color of the sample. Figure 8 shows the transformation of mineral color under different temperatures and heating/cooling paths. Below 500 ℃, the temperature and heating/cooling path have little effect on the color of the sample; Between 500 and 600 ℃, many positions of feldspar and quartz gradually turn flesh red, and some positions near cracks turn white; At 700 to 800 ℃, many positions of the SF and FF path samples gradually turn white, while the SS and FS path samples have relatively few positions that turn white. According to research and analysis, the Fe^{2+} often contained in feldspar and quartz, which is easily oxidized to Fe^{3+} at high temperature [31, 32], resulting in the sample turning red in color. After thermal crack of the rock, the development of cracks leads to the appearance of the rock turning white, which confirms why the observed white distribution is basically consistent with the distribution of cracks. Therefore, the color of the sample turning red is an allochromatic color, and turning white is a false color.

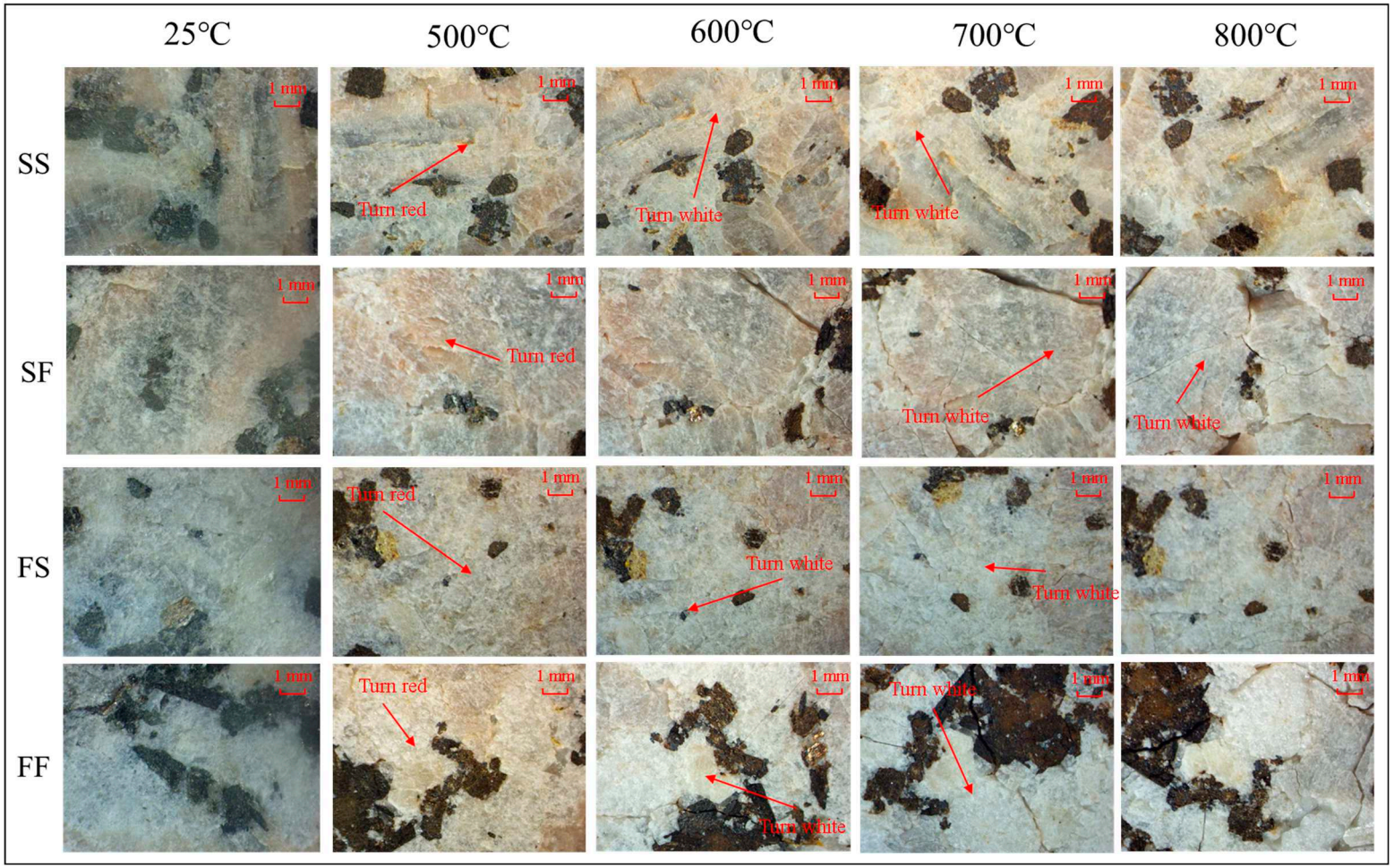

Figure 8. Microscopic changes of samples under four heating/cooling paths.

doi:10.20944/preprints202309.0381.v1

 doi:10.20944/preprints202309.0381.v1

Based on the above analysis, it can be concluded that the thermal fracture of granite samples under different temperatures and temperature rise and fall paths is mainly caused by thermal stress. Thermal fracture is the result of the interaction between thermal stress and rock strength. The magnitude of thermal stress is mainly affected by temperature difference, while the ability of rocks to resist damage is mainly related to hardness and shape. The magnitude of temperature difference is mainly related to the target temperature, heating/cooling rate, and the thermal conductivity of minerals. At the same target temperature, the larger the heating/cooling rate, the smaller the thermal conductivity of the mineral, which is more conducive to the formation of a large temperature difference. The ability of mineral crystals to resist damage is not only related to their strength, but also significantly influenced by their geometric shape. The higher the hardness, the smoother and more rounded the shape, and the less likely it is to be damaged. For the studied granite samples, the thermal conductivity of quartz is the highest among the main mineral components,around 7.6w/(m·K); while the difference between feldspar and hornblende is not significant, ranging from 2.2 to 3.0w/(m·K). The thermal expansion coefficient of quartz is also the largest, about 16×10-6 $℃^{-1}$, and there is also not much difference between feldspar and hornblende,range 4×10-6 $℃^{-1}$ to 7×10-6 $℃^{-1}$. From the hardness perspective, the Mohs hardness of quartz is 7, feldspar is generally 6, and the hornblende is between 5 and 6. From the perspective of mineral morphology, hornblende aggregates are the smallest, mostly in block or nearly circular shapes, scattered in the sample; The aggregate of feldspar is the largest, mostly in the form of blocks or polygons, and has 2 sets of complete cleavage; Quartz finally crystallizes during the crystallization process and fills between other minerals or mineral aggregates, mainly in the form of blocks and narrow slits. Based on the above understanding of the main minerals in the sample, the mechanism of rock thermal crack can be revealed. The initial thermal cracks are generally located between the mineral particles at the edge of the sample or within the aggregate of feldspar and quartz inside the sample (as shown in Figure 9). During the heating/cooling process, the temperature gradient at the edge of the sample is relatively large. Due to the different thermal expansion and thermal conductivity between particles, the thermal stress generated by temperature gradient and stress caused by the mismatch deformation of crystal are superimposed, leading to thermal cracks between particles at the edge of the sample. The intercrystalline cracks in the quartz inside the sample mainly develop in the quartz crastal with the slit shape. Although the hardness of quartz is relatively high, the shape of the slit makes it easy for both ends of the quartz aggregate to be subjected to greater stress, resulting in certain tensile or shear cracks in the middle. The intercrystalline cracks in the feldspar inside the sample mainly develop at the cleavage position, mainly because the cleavage position is more prone to stress concentration and is also the weakest point of mineral particles. As the temperature increases, the main thermal cracks in the final crack network of SF and FF path samples mainly develop between feldspar aggregates or at the boundaries between feldspar and other mineral aggregates, while secondary thermal cracks are located in quartz or hornblende aggregates and intersect with the main thermal cracks at a large angle (Figure 9). Below 600 ℃, the main cracks mainly expanded and some discrete small cracks appeared. After 600 ℃, the cracks gradually connected and gradually formed a multi-level crack network interwoven together. This is consistent with the test results that more transgranular cracks were observed above 600 ℃. For samples under SS and FS paths, the connectivity of the thermal cracks is not strong, and large cracks are mainly developed in the middle of mineral aggregates or at the junction of different particle aggregates, and it is rare for small aggregates of amphibole particles to penetrate. This is due to the low thermal stress caused by the slow heating/cooling rate, which is not enough to cause the generated cracks to expand significantly and connect with each other, nor can they crack regular shaped hornblende blocks. This also verifies that during the temperature increase process, if the thermal expansion coefficient of the embedded particles is greater than that of the matrix, radial cracks will occur within the matrix; If the thermal expansion coefficient of embedded particles is less than that of the matrix, circumferential cracks will occur within the matrix.

The above research on the mechanism of rock thermal crack focuses on the two-dimensional crack of the sample surface. By comparing the crack ratio of the research results with the porosity

Preprints (www.preprints.org) | NOT PEER-REVIEWED | Posted: 6 September 2023 doi:10.20944/preprints202309.0381.v1

under different temperature effects in the literature (Chaki et al., 2007; Chen et al., 2017; Griffiths et al., 2017), it was found that the trend of crack ratio and porosity with temperature is very similar (as shown in Figure 10a), with a same mutation cluster region between 400 and 600 ℃. This indicates that the research results can reflect the three-dimensional fracture law of the sample to a certain extent to a certain extent. The thermal crack of rock also has certain response characteristics in macroscopic physical and mechanical properties. Previous studies have shown that P-wave velocity is a physical parameter that can better reflect thermal damage and is easy to obtain. The crack ratio during the thermal crack process in this study was compared to the changes in P-wave velocity of similar samples from published literature [33-35], and it was found that the interval where the P-wave velocity decreased faster is basically consistent with the interval where the thermal crack developed faster. Therefore, the development process of thermal cracking can be monitored through P-wave velocity. The above research can provide support for engineering monitoring technology.

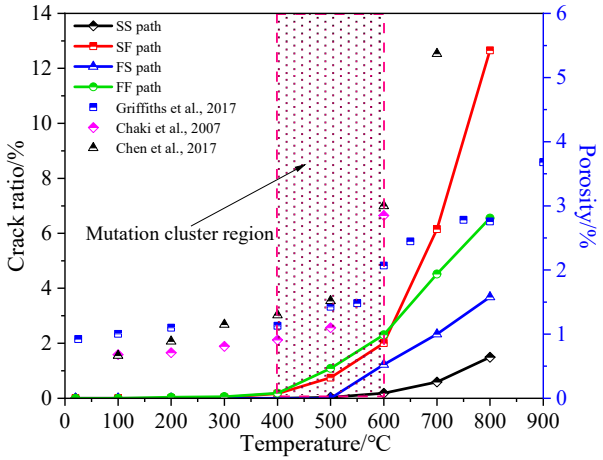

(a) Changes in thermal crack ratio and porosity with temperature

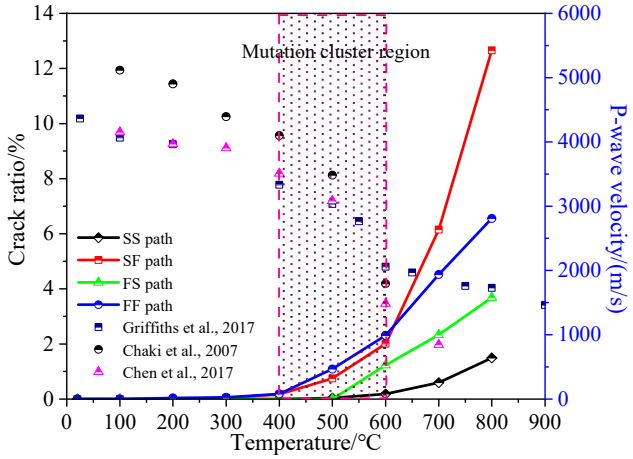

(b) Changes in thermal crack ratio and P-wave velocity with temperature

Figure 10. Relationship between crack ratio, porosity and P-wave velocity with increasing temperature [32-35].

5. Conclusions

In order to understand the thermal crack characteristics of granite that has gone through various heating/cooling processes. The surface thermal crack rate, thermal crack length, thermal crack width, thermal crack type and thermal crack characteristics of granite undergone four types of thermal treatments whose target temperatures ranged between 20-800 ℃ were studied. By comparing the previous studies on porosity and P-wave velocity of thermally damaged granite, the relationships between surface thermal crack rate and porosity and surface thermal crack rate and P-wave velocity were studied. The main findings are as follows.

1. The cooling rate of this experiment has a more significant impact on the thermal fracture of the sample than the heating rate. The rapidly cooled sample undergoes thermal cracking at around 200-300 °C, while the slowly cooled sample undergoes thermal cracking at around 600 °C. The distribution pattern of initiation positions of thermal crack in samples with different temperature paths is basically consistent, mostly located at the junction of mineral particles or irregular shapes of larger mineral aggregates. There are relatively more cracks located at the edge of the sample, and the width and length of the initiation cracks are relatively small.
2. The crack network generated by the sample with a fast cooling path at the highest test temperature is relatively complex, while the cracks of the sample with a slow cooling path are not interconnected into a network. The crack network structure of the SF path specimen is the most complex, but the size of the main crack is not as large as that of the FF path specimen, and the number of secondary cracks is more than that of the FF path specimen.
3. The thermal conductivity and thermal expansion of different mineral particles are different, leading to temperature gradients and inconsistent deformation between particles, resulting in thermal stress, tensile stress, or shear stress. They are concentrated at the boundaries of mineral aggregates, cleavage or original defects. When the total stress reaches a certain level, the main crack of thermal crack network is formed at the edges of mineral aggregates, in the middle of crystals, or between mineral particles. After the main thermal crack develops to a certain extent, smaller secondary thermal cracks will gradually develop between them, and the intersection angle between the secondary cracks and the main crack is generally larger.

Acknowledgements: This research is supported by the National Natural Science Foundation of China (Grant No. 41807233) & the Priority Academic Program Development of Jiangsu Higher Education Institutions.

Conflicts of Interest: The authors declared that they have no conflicts of interest to this work. We declare that we do not have any commercial or associative interest that represents a conflict of interest in connection with the work submitted.

References

1. Vagnon, F.; Colombero, C.; Colombo, F.; Comina, C.; Ferrero, A. M.; Mandrone, G.; Vinciguerra, S.C. Effects of thermal treatment on physical and mechanical properties of Valdieri Marble - NW Italy. *Int. J. Rock Mech. Min.* **2019**, *116*, *75-86*.
2. Chaki, S.; Takarli, M.; Agbodjan, W. P. Influence of thermal damage on physical properties of a granite rock: porosity, permeability and ultrasonic wave evolutions. *Constr. Build. Mater.* **2008**, *22*(7), *1456-1461*.
3. Daoud, A.; Browning, J.; Meredith, P. G.; Mitchell, T. M. Microstructural controls on thermal crack damage and the presence of a temperature-memory effect during cyclic thermal stressing of rocks. *Geophys. Res. Lett.* **2020**, *47*(19), *e2020GL088693*.
4. Deng, L. C.; Li, X. Z.; Wang, Y. C.; Wu, Y.; Huang, Z.; Jiang, C. L. Effect of temperature on macroscopic and microscopic properties of sandstone from Qidong coal mine. *Rock Mech. Rock Eng.* **2022**, *55*, *71-90*.
5. Ersoy, H.; Kolayli, H.; Karahan, M.; Karahan, H. H.; Sunnetci, M. O. Effect of thermal damage on mineralogical and strength properties of basic volcanic rocks exposed to high temperatures. *B. Eng. Geol. Environ.* **2019**, *78*(3), *1515-1525*.
6. Xiao, W. J.; Yu, G.; Li, H. T.; Zhang, D. M.; Li, S. J.; Yu, B. C.; Li, D. W. Thermal cracking characteristics and mechanism of sandstone after high-temperature treatment. *Fatigue Fract. Eng. M.* **2021**, *44*(11), *3169-3185*.
7. Zhang, W. Q.; Sun, Q.; Zhu, Y. M.; Guo, W. H. Experimental study on response characteristics of micro–macroscopic performance of red sandstone after high-temperature treatment. *J. Therm. Anal. Calorim.* **2019**, *136*, *1935-1945*.
8. Zhang,S.K; Huang, Z.W; Zhang, H.Y; Guo,Z.Q; Wu, X.G; Wang, T.Y; Zhang, C.C; Xiong, C. Experimental study of thermal-crack characteristics on hot dry rock impacted by liquid nitrogen jet. *Geothermics* **2018**, *76 , 253-260*.
9. Zhang, W.Q.; Sun, Q.; Hao, S. Q.; Geng, J. S.; Lv, C. Experimental study on the variation of physical and mechanical properties of rock after high temperature treatment. *Appl. Therm. Eng.* **2016**, *98*, *1297-1304*.
10. Huang, Z.; Zeng,W.; Gu, Q.X; Wu,Y.; Zhong, W.; Zhao, Kui. Investigations of variations in physical and mechanical properties of granite, sandstone, and marble after temperature and acid solution treatments. *Constr. Build. Mater.* **2021**, *307, 124943*.
11. Shen, Y. J.; Hou, X.; Yuan, J. Q.; Wang, S. F.; Zhao, C. H. Thermal cracking characteristics of high-temperature granite suffering from different cooling shocks. *Int. J. Fracture* **2020**, *225*, *153-168*.
12. Sirdesai, N. N.; Mahanta, B.; Ranjith, P. G.; Singh, T. N. Effects of thermal treatment on physico-morphological properties of Indian fine-grained sandstone. *B. Eng. Geol. Environ.* **2019**, *78*(2), *883-897*.

13. Chen,T.T.; Foulger, G.R.; Tang, C.A; Mathias, S.A.; Gong, Bin. Numerical investigation on origin and evolution of polygonal cracks on rock surfaces. *Eng. Geol.* **2022**, *311, 106913.*
14. Wu, Z.Y.; Jiao, Y.Y.; Zheng, F.; Huang, G.H.;, Liu, C.D. A new SDDA-based numerical approach for simulating rock cracking induced by temperature stresses. *Comput. Geotech.* **2023**, *154, 105113.*
15. Wang, Z.W.; Liu, Q.S.; Wang, Y.X. Thermo-mechanical FDEM model for thermal cracking of rock and granular materials. *Powder Technol.* **2021**, *393, 807-823.*
16. Liua, J.R.; Li, B.Y.; Tian,W.; Wu, X.R. Investigating and predicting permeability variation in thermally cracked dry rocks. *Int. J. Rock Mech. Min.* **2018**, *103, 77-88.*
17. Zhao, Y. S.; Feng, Z. J.; Zhao, Y.; Wan, Z. J. Experimental investigation on thermal cracking, permeability under HTHP and application for geothermal mining of HDR. *Energy* **2017**, *132, 305-314.*
18. Zhang, F.; Zhao, J. J.; Hu, D. W.; Frederic, S.; Shao, J.F. Laboratory Investigation on physical and mechanical properties of granite after heating and water-cooling treatment. *Rock Mechan. Rock Eng.* **2018**, *51, 677-694.*
19. Feng, Z. J.; Zhao, Y. S.; Zhang, Y.; Wan, Z. J. Real-time permeability evolution of thermally cracked granite at triaxial stresses. *Appl. Thermal Eng.* **2018**, *133, 194-200.*
20. Freire-Lista, D. M.; Fort, R.; Varas-Muriel, M. J. Thermal shock-induced microcracking in building granite. *Eng. Geol.* **2016**, *203, 83-93.*
21. Zhang, W. Q.; Sun, Q.; Hao, S. Q.; Wang, B. Experimental study on the thermal damage characteristics of limestone and underlying mechanism. *Rock Mech. Rock Eng.* **2016**, *49, 2999-3008.*
22. Yang, J.C.; Cheng, Y.F.; Han, S.C; Yan,C.L.; Xue, M.Y.; Ding, J.P.; Chen, F.Y. Research on the characteristics of crack propagation at high temperatures based on digital image correlation technology. *Eng.g Fract. Mech.* **2022**, *263, 108295.*
23. Jiang,Y.F.; Zhu,Z.M.; Yu,L.Y; Zhou,L.; Zhang,R.F.; Ma, L.J. Investigation of the fracture characteristics of granite and green sandstone under different thermal treatments.*Theor. Appl. Fract. Mec.* **2022**, *118, 103217.*
24. Shao, S. S.; Ranjith, P. G.; Wasantha, P. L. P.; Chen, B. K. Experimental and numerical studies on the mechanical behaviour of Australian Strathbogie granite at high temperatures: An application to geothermal energy. *Geothermics* **2015**, *54, 96-108.*
25. Wang, F.; Konietzky, H. Thermo-Mechanical Properties of Granite at Elevated Temperatures and Numerical Simulation of Thermal Cracking. *Rock Mech. Rock Eng.* **2019**, *52, 3737-3755.*
26. Mambou, L. L. N.; Ndop, J.; Ndjaka, J. M. B. Theoretical investigations of mechanical properties of sandstone rock specimen at high temperatures. *J. Min. Sci.* **2014**, *50(1), 69-80.*
27. Zhao, G. J.; Chen, C.; Yan, H.; Hao, Y. L. Study on the damage characteristics and damage model of organic rock oil shale under the temperature effect. *Arab. J. Geosci.* **2021**, *14(8), 722.*
28. Tang, X.H.; Tao, S.J.; Li,P.; Rutqvist,J.; Hu,M.S.; Sun, L. The propagation and interaction of cracks under freeze-thaw cycling in rock-like material. *Int. J. Rock Mech. Min.* **2022**, *154, 105112.*
29. Jiang,Y.F.; Zhou,L.; Zhu,Z.M.; Ma,L.J.; Chen,J.X.; Li, Y.J. Research on dynamic cracking properties of cracked rock mass under the effect of thermal treatment. *Theor. Appl. Fract. Mec.* **2022**, *122, 103580.*
30. Li, W.; Chen; W.H. Linear crack initiation analysis on rock surface under the combined action of sub-elevated temperature stress and fracture air-vapor pressure. Theor. Appl. Fract. Mec. **2022**, *122, 103582.*
31. Liu, W.J.; Zhu, X.H.; Lv, Y.X; Tong, H. On the mechanism of thermally induced micro-cracking assisted rock cutting in hard formation. J. Petrol. Sci. Eng. **2021**, *196, 107666.*
32. He,Q.; Chen,S.W.; Wang, G.B.; Zuo, S.Y.; Yang, F.B. Evolution of thermal cracking, temperature distribution and deformation at mineral scale of Beishan granite during heating and cooling. Int. Commun. Heat Mass **2023**, *144, 106781.*
33. Chen, S. W.; Yang, C. H.; Wang, G. B. Evolution of thermal damage and permeability of Beishan granite. *Appl. Therm. Eng.* **2017**, *110, 1533-1542*.
34. Chaki, S.; Takarli, M.; Agbodjan, W. P. Influence of thermal damage on physical properties of a granite rock: porosity, permeability and ultrasonic wave evolutions. *Constr. Build. Mater.* **2008**, *22(7), 1456-1461*.
35. Griffiths, L.; Heap, M. J.; Baud, P.; Schmittbuhl, J. Quantification of microcrack characteristics and implications for stiffness and strength of granite. *Inter. J.Rock Mech. Min.* **2017**, *100, 138-150*.